

# Consolidation of AA 7075 – 2 wt.% ZrO<sub>2</sub> composite powders by severe plastic deformation via ECAP

S. E. Hernández-Martínez<sup>1,\*</sup>, J. J. Cruz-Rivera<sup>1</sup>, R. Martínez-Sánchez<sup>2</sup>, C.G. Garay-Reyes<sup>2</sup>, J.A. Muñoz-Bolaños<sup>3</sup>, J.M. Cabrera<sup>3,4</sup>, J. L. Hernández-Rivera<sup>5</sup>.

<sup>1</sup> Instituto de Metalurgia, Universidad Autónoma de San Luis Potosí, Sierra Leona No.550, Unidad de Posgrados, San Luis Potosí, S.L.P., México.

<sup>2</sup> Centro de Investigación en Materiales Avanzados (CIMAV), Miguel de Cervantes No.120, Chihuahua, Chih., México.

<sup>3</sup> Universitat Politècnica de Catalunya, Departamento de Ciencia de Materiales e Ingeniería Metalúrgica, Av. Diagonal, 647- 08028 Barcelona, Spain

<sup>4</sup> Fundación CTM Centro Tecnológico, Plaza de la Ciencia 2, 08243 Manresa, Spain

<sup>5</sup> CONACYT Research Fellow-Instituto de Metalurgia, Universidad Autónoma de San Luis Potosí-, Sierra Leona No.550, San Luis Potosí, S.L.P., México

.

## 1. Introduction

The combination between low specific weight and high mechanical strength of aluminium based composites has increased the interest for its development in the aeronautic industry. The superior mechanical strength can be achieved by dispersing hard ceramic particles through the matrix, promoting the so-called Oxide Dispersion Strengthening (ODS materials) [1,2]. There are several methods for composites production But one of the techniques that have showed higher efficiency to disperse ceramic particles is the mechanical milling (MM), since the process is held completely in solid state, contrary to liquid state methods, where a difference in density between matrix and particles makes difficult the dispersion of the reinforcement phase [3]. On the other hand, one of the novel methods for powder consolidation is the Equal Channel Angular Pressing (ECAP), which has shown superior mechanical properties of the final consolidated material; moreover, a better dispersion can be achieved since the deformation process involves large strain regardless of matrix and reinforcement particle sizes and volume fractions [4-6]. One of the advantageous features of ECAP is that there is no reduction in the cross section of the sample [7]. In addition, ECAP requires lower pressure and temperature in comparison with hot extrusion [5]. Often, further deformation processes are used in the production of aluminum based composites to enhance dispersion and density of the composite [8-10].

Previous studies have used ZrO<sub>2</sub> as reinforcement particles with the aim of improving the strength properties of the aluminum. Fuentes-Ramirez *et al.* [11] improved the wear resistance of pure Al, using a surface treatment employing colloidal ZrO<sub>2</sub>. In other research, Hemanth [12] used nanosized ZrO<sub>2</sub> to modify LM13 cast aluminum alloy, obtaining superior properties of hardness and tensile strength in comparison with the unreinforced alloy. In the same way, Abdizadeh *et al.* [13] reinforced an A365 aluminum alloy with partially yttria-stabilized zirconia by the vortex method, reaching a hardness of 70 HBN and tensile strength of 240 MPa, while the unreinforced

material exhibited values of 45 HBN and 45 MPA, respectively. Dutkiewicz *et al.* [14] used an aluminum alloy 7475 using ZrO<sub>2</sub> with an average size of 20 nm, obtaining a compressive stress near to 990 MPa.

The aluminum alloy AA 7075 is considered a high strength alloy, since its yield point is over 500 MPa [15,16]. On the other hand ZrO<sub>2</sub> is a hard ceramic [17,18] which is thought to promote superior mechanical properties to the alloy in comparison with the unreinforced one. Unfortunately, it is showed an undesirable reaction between ZrO<sub>2</sub> and the alloying elements, when the powders are consolidated by traditional powder metallurgy routes, such as sintering and hot extrusion (400 and 500 °C respectively). Under this condition, Intermetallic phases are formed and a depletion of the solute in the matrix is caused. Hence, the alloy will not be capable to display age hardening, since there is no solute to form  $\eta'$  and  $\eta$  (MgZn<sub>2</sub>) phases. Therefore, high temperature processes are no longer an option to reinforce AA 7075 with ZrO<sub>2</sub> particles. Encouraged by this situation, a low temperature ECAP processing is proposed as an alternative powder consolidation process, in order to avoid the mentioned reaction and to take advantage of the additional ECAP benefits, namely, the strengthening mechanism induced by severe plastic deformation in addition to the mechanical milling.

## 2. Experimental

The initial matrix powders were obtained from a commercial bar of AA 7075 supplied in T6 state. The bar was annealed during 48 h at 415 °C with the purpose of removing the T6 aging treatment. The bar was grinded and then, the obtained burrs were sieved using 50 mesh size. The yttria-stabilized zirconia particles used in this research were previously milled in a planetary ball mill for 80 h, reaching an average size of 110 nm. The ZrO<sub>2</sub> particles had an irregular shape and consisted of a mixture of 63 and 37 wt.% of monoclinic and tetragonal structures respectively according to [19]. The composite was produced by blending the AA 7075 with 2 wt.% of ZrO<sub>2</sub> particles, and then mechanically milled in a horizontal attritor Simoloyer by 15 h. Stainless steel balls were employed as the milling media in a ball-to-powder ratio of 20:1 and 1.5 mL of methanol was used as process control agent (PCA). Milling was performed at 1000 rpm and more detail of the process can be found elsewhere [20].

The composite powders were cold compacted inside AA 6061 tubes by employing a Universal Testing Machine SHIMADZU AG-I. This process was performed by steps until a load of 196 kN was reached. The tubes (with the powders inside) were subjected to ECAP process in order to get a fully consolidated material. For this purpose an ECAP die with an inner and outer angle of 90° and of 37°, respectively, was used, applying a ram speed of 4 mm per minute at two conditions, namely, room temperature and at 220 °C, in the same universal testing machine. The composite microstructure was characterized via electronic microscopy in a Phillips XL-30 Scanning Electron Microscope (SEM) operated at 20 kV and in a JEOL 1230 Transmission Electron Microscope (TEM) operated at 100 kV. In both microscopes, Dispersion Spectroscopy (EDS) analysis was used in order to determine the chemical composition of the different phases obtained in the samples. The structural features and phase identification were determined by X-Ray Diffraction (XRD) in a Bruker D8 Advance Dvinci Design diffractometer, in the 2 $\theta$  range of 25–85°, using Cu radiation K $\alpha$  ( $\lambda$  = 0.154 nm), with a step-size of 0.02° and speed of 1°/min. Vickers hardness tests for the powders and consolidated materials

were performed in accordance to ASTM E92 standard. The image analyzer software Sigma ScanPro 4.0 was used in order to quantify the remaining porosity of the consolidated material using SEM micrographs. Additionally, studies via Differential Scanning Calorimetry (DSC) were carried out to the metallic powders, with the aim of understanding the nature of the precipitation and phase transformations taking place into the composite system. The DSC tests were performed in a Seratam Labsys Evo, with a heating rate of 10 °C/min, from room temperature until 550 °C.

### 3. Results

#### 3.1 Consolidation by ECAP

The mechanism of powder consolidation by ECAP process is believed to act in the following way: initially, the load exercised on the powders diminished the distance between particles promoting an intimate contact (it is understood that this compaction is additional because the powders have been previously compacted when the tube was closed). Then when the powders were passing through the shear plane in the ECAP die, the shear stresses break the oxide layer in the surface of aluminum particles, exposing fresh surfaces. As a consequence, these surfaces come in contact, and inter-particle welding occurs due to both applied stress and heat generated, consolidating the powders and resulting into a bulk material [4,5].

In order to fully understand the process of powder consolidation inside the tubes, Figure 1 presents the load-displacement curve obtained during the ECAP process. According to [4], in the very beginning, the load increases due to further compaction of powders and also because of the friction between tube and die walls. The maximum load is reached when the yield point of the front part of the tube is achieved. Once this point is overpassed, the load decreases until a minimum as the tube and powder pass completely throughout the shear plane. This load drop is expected since the load requirements are lower for deforming powder instead of bulk material. The load starts to increase at 32 mm of displacement when the friction between the wall and the exit channel becomes significant; furthermore, in this moment the upper part of the tube (rear plug) starts its entrance to the shear plane.

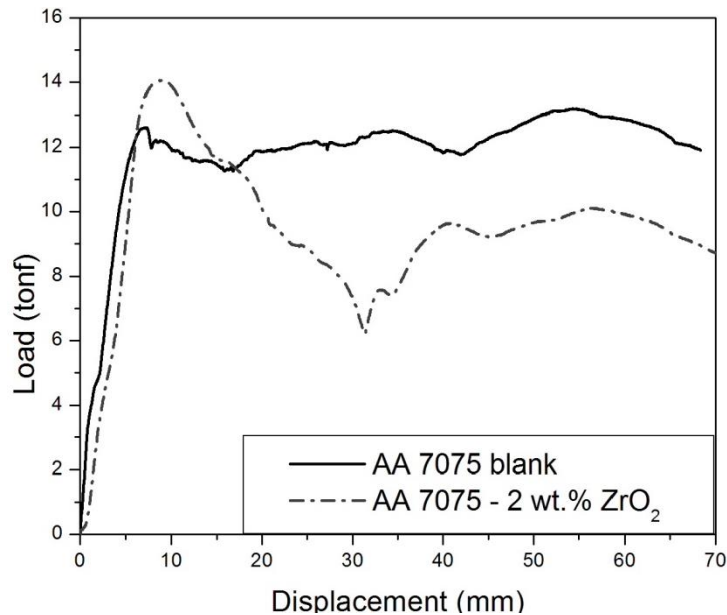


Figure 1. Load- displacement curve of the AA 7075 – 2 %wt. ZrO<sub>2</sub> consolidation process by single ECAP pass.

One of the most important features in evaluating the ECAP process when used as metal powder consolidation process is the remaining porosity. The result of a poor consolidation process is a significant porosity in the material, and this can lead in most cases to detrimental mechanical properties [21].

SEM micrographs of the consolidated powders with different number of passes by ECAP and working temperature are shown in Fig. 2. One can notice that the use of high temperature improves the reduction of porosity in the composite. The pores are higher in number and also in size when ECAP is conducted at room temperature, while porosity is reduced when ECAP is performed at 220°C as illustrated in Figs 2a and 2b respectively.

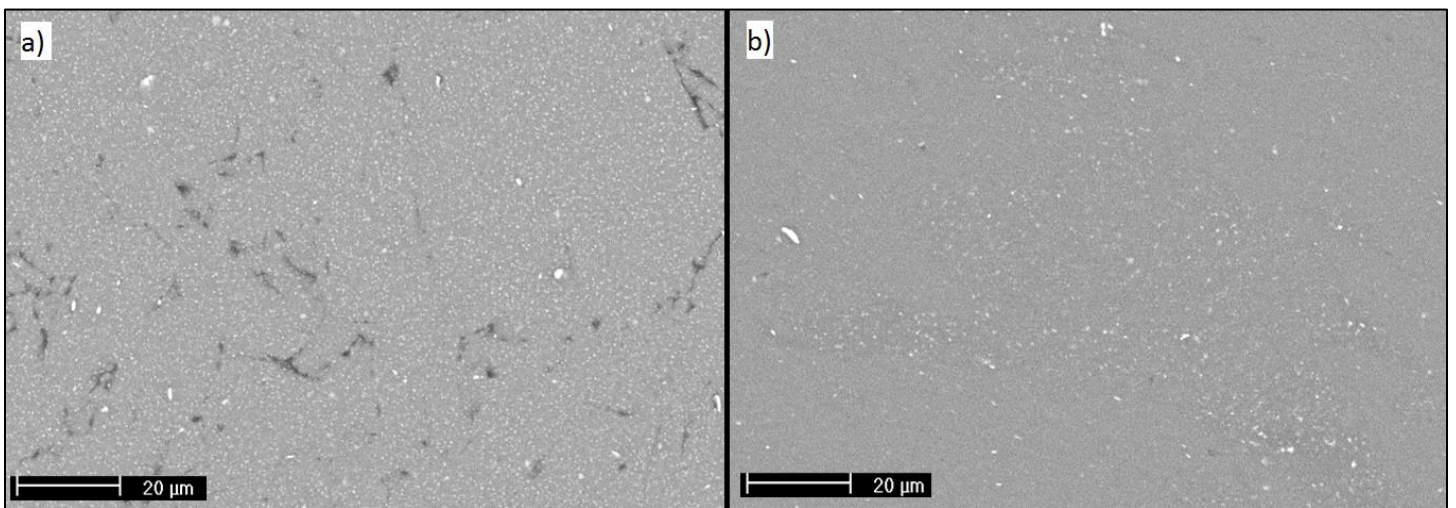


Figure 2. SEM micrographs of AA 7075 – 2 wt.% ZrO<sub>2</sub> composite a) consolidated by 3 ECAP passes at room temperature, and b) consolidated by a single ECAP pass at 220 °C.

Porosity was evaluated by image analysis through Sigma ScanPro software. Results are listed in Table I. The powders consolidated at room temperature by three ECAP passes have a remaining porosity value of 1.9% and the powders consolidated at 220 °C by one single ECAP pass have a 0.1%. This finding can be explained by two facts. First the heat generated by plastic deformation activates the inter-particle diffusion similar to conventional sintering but at a lower temperature and a shorter time. And second, the metallic powders of the composite have a slightly recovery ought to the heat generated, and this softening enhanced the inter-particle bonding of the previously hard milled powders which were difficult to being welded at room temperature.

Table I. Remaining porosity of the AA 7075 and the composite at different conditions.

Condition	Remaining Porosity
AA 7075 – 2% ZrO <sub>2</sub> / 3 pass - Room temperature	1.9%
AA 7075 powder / 1 pass - 220 °C	0.4%
AA 7075 – 2% ZrO <sub>2</sub> / 1 pass - 220 °C	0.1 %

Another parameter to evaluate the consolidation process is the hardness. Accordingly, the Vickers hardness values of the unreinforced alloy and the composite at different processing conditions are listed in Table II. The first interesting finding is that the sample processed by ECAP at high temperature offers similar hardness than in the case of the unreinforced aged alloy. In this way, it seems that the mechanical properties are enhanced by this processing route. The influence of the processing temperature is also visible on the composite material processed at room temperature by three ECAP passes since it exhibits only 161 HVN which is below of the hardness peak of the commercial aged alloy. When the composite processed by ECAP at 220 °C is compared with all other conditions, it is clearly seen that the value of hardness is higher than at all other samples. This fact can be taken as an assertion of the hypothesis assumed earlier regarding that the bonding between particles has been further improved with usage of temperature. It can also be seen that the HVN value from the composite in powder condition is higher than the value in the powder condition at room temperature. This can be associated to the presence of relatively large porosity in the consolidated condition

Table II. Vickers hardness of the AA 7075 and the composite at different conditions.

Condition	Vickers hardness (HVN)
AA 7075 commercial supersaturated solid solution	88
AA 7075 commercial hardness peak (aged condition T6)	184
AA 7075 powders (after mechanical milling)	254
AA 7075 - 2 wt.% ZrO <sub>2</sub> powders (after mechanical milling)	281
AA 7075 – 2 wt.% ZrO <sub>2</sub> / 3 pass ECAP at room temperature	161
AA 7075 – 2 wt.% ZrO <sub>2</sub> / single pass ECAP at 220 °C	257

TEM micrographs for the AA 7075 - 2 wt.% ZrO<sub>2</sub> composite material consolidated by single ECAP pass process at 220° C are shown in Figure 3, where the interaction between ZrO<sub>2</sub> particles and the metal matrix

can be noticed. Figure 3a corresponds to a bright field micrograph, while Figure 3b corresponds to dark field image taken from the the arrowed point in the selected area electron diffraction pattern (plane (111) of the metal matrix) also indicated in Figure 3b.. It can be noted that there is absence of reinforcement clusters in the matrix and the distribution of reinforcement particles appears homogenous, supporting the statement made by Tan and Zhang [8] and Saabirov et al. [9,10], who suggested that increased deformation leads to a good dispersion of reinforcement particles, It can also be seen in Figure 3b that the crystallites are visible to be small enough to declare them as nanosized, according to [23].

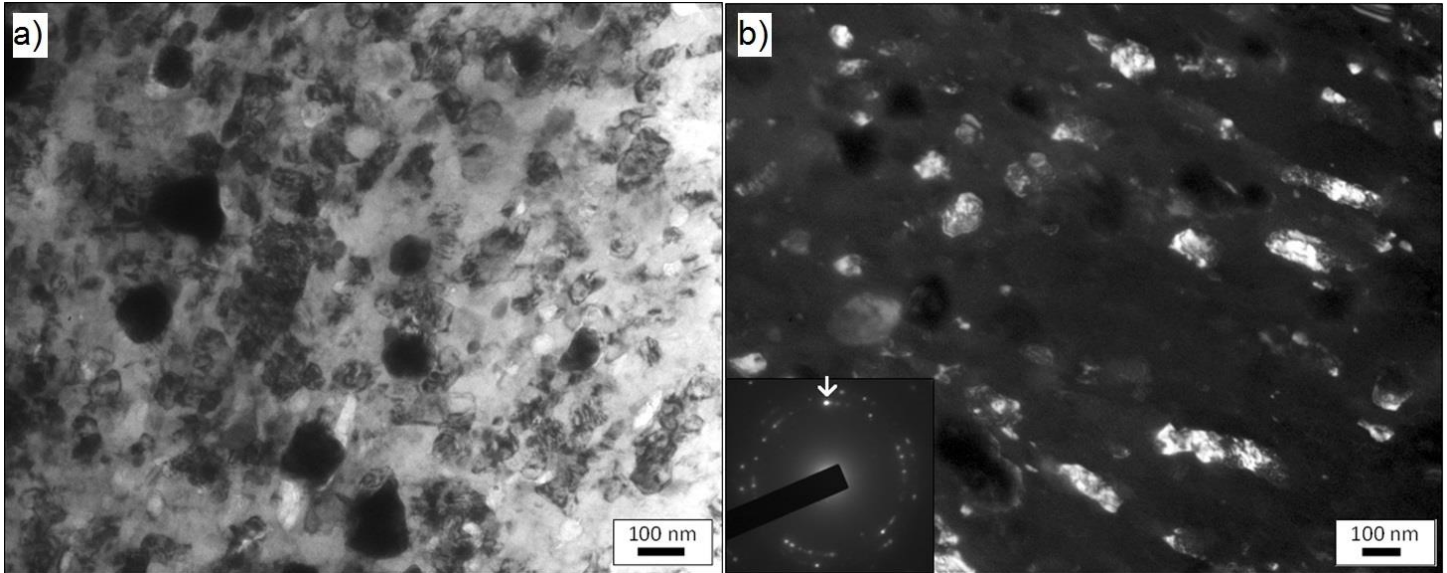


Figure 3. TEM micrographs of the AA 7075 – 2 wt.% ZrO<sub>2</sub> mechanically milled and consolidated by ECAP at 220 °C.

### 3.2 Comparison between ECAP consolidation and sintering- hot extrusion of the system AA 7075 – ZrO<sub>2</sub>.

In this section additional relevant arguments are given to explain why the ECAP process possess significant benefits for consolidation of AA 7075 – ZrO<sub>2</sub> on contraposition to the disadvantages showed when sintered and/or hot extruded at high temperatures (400 and 500 °C, respectively). The aging curves of the bulk AA 7075 (commercial) and the AA 7075 – 2 wt.% ZrO<sub>2</sub> composite consolidated by sintering and hot extrusion are shown in Fig. 5. It is evident that the response of the composite to the precipitation heat treatment is negligible. This lack of hardening is proposed to be an adverse reaction between the ZrO<sub>2</sub> particles and the alloying elements of the matrix (Zn basically). In this way, when the composite is processed at high temperature, new intermetallic phases are formed, leaving the matrix depleted in solute. Therefore, there is not enough solute to form GP zones and  $\eta'$  (MgZn<sub>2</sub>) precipitates and the material will not harden.

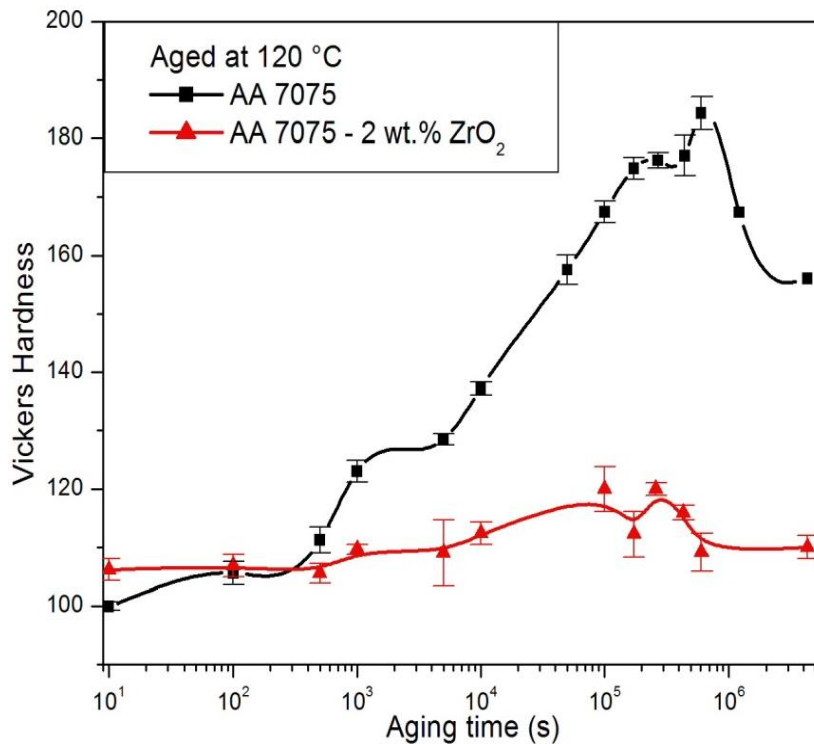


Figure 4. Variation of hardness with aging time for AA 7075 and the AA 7075 – 2 wt.% ZrO<sub>2</sub> composite sintered and hot extruded. [refs]

These new phases were identified by X- ray diffraction and are presented in Figure 5 where the diffractogram of the composite powders in the as milled condition, and the one corresponding to composite after consolidation by sintering and hot extrusion are compared. It is apparent that the peaks of the MgZn<sub>2</sub> and ZrO<sub>2</sub> phases disappeared or lowered their intensity after sintering and extrusion. As well new peaks are formed after this processing route. It is stated that these intermetallic phases (presented in the Table III) are responsible for solute depletion in the matrix.

Table III. Intermetallic phases formed during high temperature processes in the composite system AA 7075 – ZrO<sub>2</sub>.

Phase	Structure	JCPDS-card
Zn <sub>0,865</sub> Mg <sub>0,73</sub> Al <sub>10,27</sub> O <sub>17</sub>	Rombohedral	76-2464
Zn <sub>22</sub> Zr	Cubic	65-6202
Al <sub>2</sub> ZnZr	Cubic	65-4732

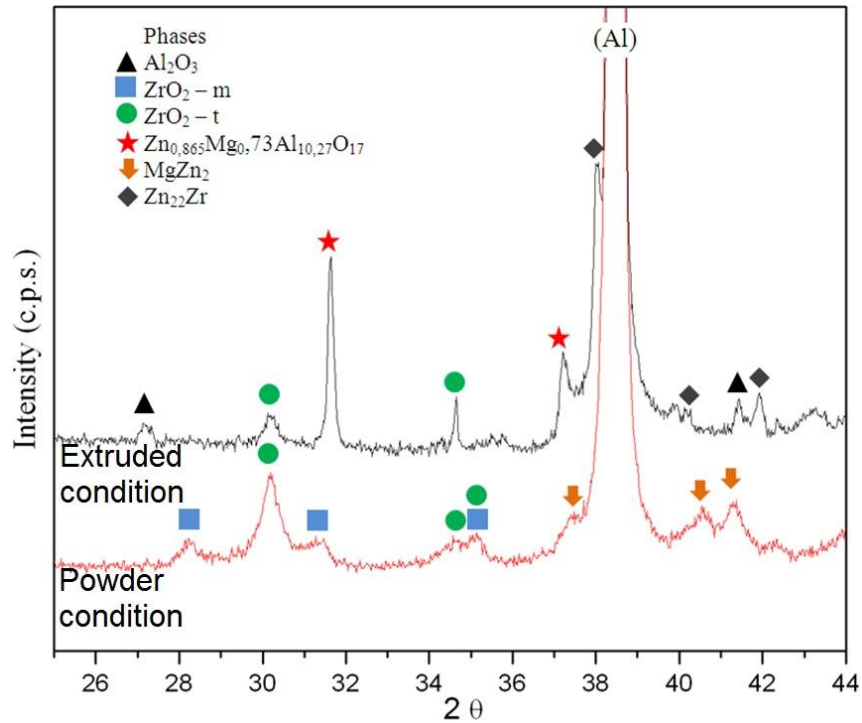


Figure 5. X-ray diffraction pattern of AA 7075 - 2 wt.%  $\text{ZrO}_2$  composite powder in the as milled condition and after sintering and hot extrusion condition

On Figure 6, it is presented a comparison between X-ray diffraction patterns of the sintered and hot extruded composite and the one processed by ECAP at  $220^\circ\text{C}$ . It is clear that there is no formation of new phases in the second case since there is no evidence of diffraction peaks corresponding to new phases as in the case of hot extruded sample. Furthermore, it is apparent that peak intensity of the ECAP processed sample is lower in comparison to the extruded material, which is a consequence of the severe plastic deformation imposed to this composite.

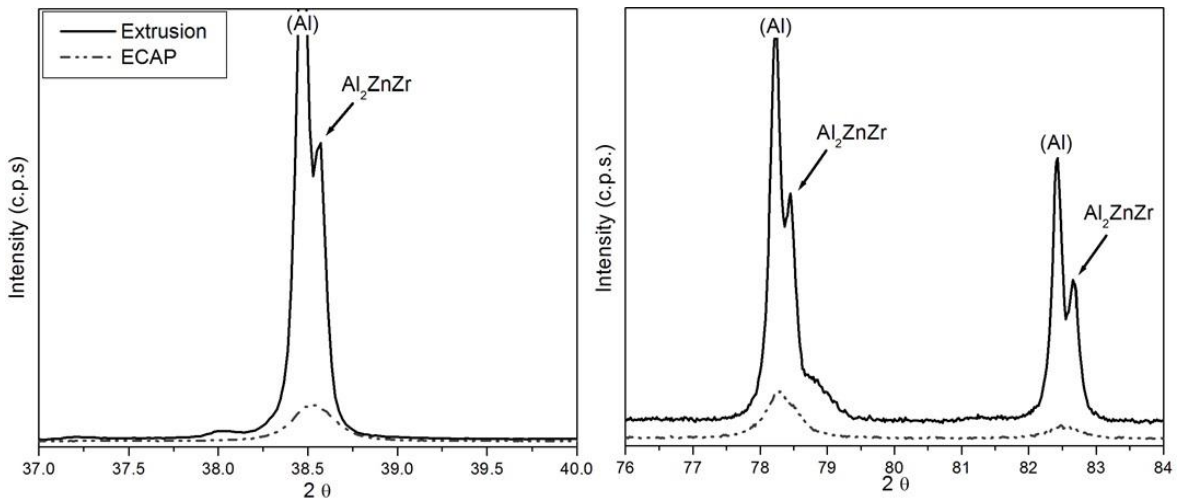


Figure 6. X-ray diffraction pattern of 7075 - 2 wt.%  $\text{ZrO}_2$  composite processed by sintering and hot extrusion and single pass ECAP at  $220^\circ\text{C}$ .

In Figure 7 it is presented a DSC thermogram of the mechanically milled powders of the AA 7075 with and without reinforcement. It is evident that there is a clear difference between the curve of the alloy and the

composite powders. The main difference remains in the temperatures between 349 to 430 °C, where an exothermic peak is noticed in the case of the composite, which is not present in the unreinforced alloy curve. Also, around 480 °C there is another peak, endothermic in this case, which is not observed in the blank sample curve. These mentioned peaks are believed to represent the different reactions of formation of the intermetallics phases mentioned in Table III.

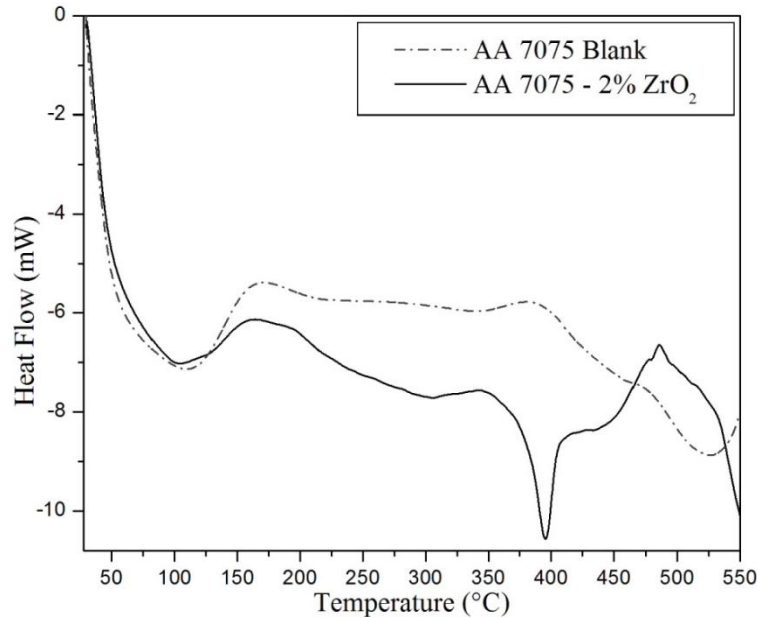


Figure 7. DSC thermogram of the powders of the mechanically milled AA 7075 powders, and the powders of the AA 7075 – 2 %wt. ZrO<sub>2</sub> composite.

According to the precipitation reaction of the AA-7075 alloy, and in agreement with [24-26], the peaks found between 100 and 150 °C are due to the dissolution of GP zones and formation of  $\eta'$  precipitates particles. It is worth to mention that these processes can be overlapped, *i.e.*, a precipitation reaction is not already finished when another has begun (collateral reactions). For example, in the range between 150 and 250 °C formation and growth of  $\eta'$  takes place, but also the formation of  $\eta$  phase. At this temperature and forward,  $\eta$  precipitates grow until its dissolution which begins at 300 °C, reaching its maximum peak at 380 °C. The precipitation reactions mentioned are not noticed in the thermogram curve for the composite material, since reaction between ZrO<sub>2</sub> and alloying elements are taking place in the composite. With the results mentioned earlier, a useful working temperature below 300 °C can be defined for a successful performance of the composite in subsequent processes.

## Acknowledgements

The present research work was supported by Universidad Autónoma de San Luis Potosí, Centro de Investigación en Materiales Avanzados Unidad Chihuahua and Universitat Politècnica de Catalunya, and financial support by CONACYT is appreciated. A special acknowledgment is extended to Claudia Elias, Rosalina Tovar and Ana Hernández Expósito (from Fundacio CTM Centre Tecnològic) for the technical assistance.

## Conclusions

1. It has been possible to obtain a fully dense composite material based on an Aluminum Alloy 7075 reinforced with  $ZrO_2$  dispersed by combining the plastic deformation of mechanical milling with other severe plastic deformation process like ECAP at 220 °C.
2. The ECAP was carried out at lower temperature and with minor load requirements, in comparison with traditional sintering and hot extrusion processes, thus, the temperature of the process is low enough to avoid reaction between reinforcement particles and the alloying elements of the AA-7075.
3. The usage of temperature in the ECAP process enhanced the consolidation process, obtaining a lower value of remaining porosity percentage and a higher Vickers hardness than the composite processed at room temperature.
4. The hardness values of the consolidated composite material by ECAP are higher than the commercial aged AA-7075 alloy .

## References

- [1] J.S. Benjamin, M.J. Bomford, Dispersion strengthened aluminum made by mechanical alloying, *Metall. Trans. A* 8A (1977) 1301–1305.
- [2] El-Eskandarany, *Mechanical Alloying for Fabrication and Advanced Engineering Materials*, William Andrew Publishing, New York, 2001.
- [3] C. Suryanarayana, Mechanical alloying and milling, *Prog. Mater. Sci.* 46 (2001) 1–184.
- [4] A.V. Nagasekhar, Y. Tick-Hon, K.S. Ramakanth, Mechanics of single pass equal channel angular extrusion of powder in tubes, *Applied Physics A* 85 (2006) 185.
- [5] Derakhshandeh, S.A. Jenabali, A. Moresedgh, M. Tabandeh, A comparison between ECAP and conventional extrusion for consolidation of aluminum metal matrix composite, *Journal of Materials Engineering and Performance* 21 (2012) 1885.
- [6] K. Xia, X. Wu, Back pressure equal channel angular consolidation of pure Al particles, *Scripta Mater.* 53 (2005) 1225-1229
- [7] V.M. Segal, Materials processing by simple shear, *Mater. Sci. Eng. A* (1995) 157.
- [8] M.J. Tan, X. Zhang, Powder metal matrix composites: selection and processing, *Mater. Sci. Eng. A* 224 (1998) 80.
- [9] I. Sabirov, O. Kolednik, R.Z. Valiev, R. Pippan, Equal channel angular pressing of metal matrix composites: effect on particle distribution and fracture toughness, *Acta Mater.* 53 (2005) 4919.

- [10] I. Sabirov, O. Kolednik, R. Pippan, Homogenization of metal matrix composites by high-pressure torsion, *Met. Mater. Trans. A* 36 (2005) 2861.
- [11] R. Fuentes-Ramirez, A. Perez-González, V.M. Castaño-Meneses, Improved wear resistance of an aluminum-zirconia composite, *Met. Sci. Heat Treat.* 52 (2010) 368.
- [12] J. Hemanth, Development and property evaluation of aluminum alloy reinforced with nano-ZrO<sub>2</sub> metal matrix composites (NMMCs), *Mater. Sci. Eng. A* 507 (2009) 110.
- [13] H. Abdizaeh, M.A. Baghchesara, Investigation on mechanical properties and fracture behaviour of A356 aluminum alloy based ZrO<sub>2</sub> particles reinforced metal-matrix composites, *Ceram. Int.* 39 (2013) 2045.
- [14] J. Dutkiewicz, L. Litynska-Dobrzynska, K. Matsuda, Structure of composites consolidated from ball milled 7475 aluminum alloy and ZrO<sub>2</sub> powders, *Int. J. Mater. Res.* 104 (2013) 123–128.
- [15] J.K. Park, A.J. Ardell, Microstructures of the commercial 7075 Al alloy in the T651 and T7 tempers, *Metall. Trans. A* 14A (1983) 1957.
- [16] A.K. Mukhopadhyay, Microstructure and properties of high strength aluminum alloys for structural applications, *Trans. Indian Inst. Metals* 62 (2009) 113.
- [17] T.K. Gupta, J.H. Bechtold, R.C. Kuznicki, L.H. Cadoff, B.R. Rossing, Stabilization of tetragonal phase in polycrystalline zirconia, *J. Mater. Sci.* 12 (1977) 2421–2426.
- [18] M.H. Bocanegra-Bernal, S. Díaz de la Torre, Review phase transitions in zirconium dioxide and related materials for high performance engineering ceramics, *J. Mater. Sci.* 37 (2002) 4947.
- [19] S.E. Hernández-Martínez, J.J. Cruz-Rivera, C.G. Garay-Reyes, C.G. Elias-Alfaro, R. Martínez-Sánchez, J.L. Hernández-Rivera, Application of ball milling in the synthesis of AA 7075–ZrO<sub>2</sub> metal matrix nanocomposite, *Powder Technol.* 284 (2015) 40.
- [20] S.E. Hernández-Martínez, J.J. Cruz-Rivera, C.G. Garay-Reyes, R. Martínez-Sánchez, I. Estrada-Guel, J.L. Hernández-Rivera, Comparative study of synthesis of AA 7075–ZrO<sub>2</sub> metal matrix composite by different mills, *J. Alloys Compd.* 643 (2015) S107.
- [21] J.B. Fogagnolo, M.H. Robert, E.M. Ruiz-Navas, J.M. Torralba, 6061 Al reinforced with zirconium diboride particles processed by conventional powder metallurgy and mechanical alloying, *J. Mater. Sci.* 39 (2004) 127.
- [23] Z. Horita, T. Fujinami, M. Nemoto, T. Langdon, Equal-channel angular pressing of commercial aluminum alloys: Grain refinement, thermal stability and tensile properties, *Metall. Mater. Trans. A*, 31 (2000) 691.
- [24] R. Delasi, P.N. Adler, Calorimetric studies of 7000 series aluminum alloys: I. Matrix precipitate characterization of 7075, *Metall. Trans.* 8A (1977) 1177.

- [25] P.N. Adler, R. Delasi, Calorimetric studies of 7000 series aluminum alloys: II. Comparison of 7075, 7050 and RX720 alloys, Metall. Trans. 8A (1977) 1185.
- [26] D.J. Lloyd, M.C. Chaturvedi, A calorimetric study of aluminum alloy AA-7075, J. Mater. Sci. 17 (1982) 1819.
- [27] K.S. Ghosh, N. Gao, Determination of kinetic parameters from calorimetric study of solid state reactions in 7150 Al-Zn-Mg alloy, Trans. Nonferrous Met. Soc. China 21 (2011) 1199.